Simulation of Tsunami impact upon Coastline

Aristotelis Spathis-Papadiotis[1] and Konstantinos Moustakas[1]

Electrical and Computer Engineering Department
University of Patras, Patra, Greece
moustakas@upatras.gr

Abstract. This paper presents a simulation of a tsunami impact upon an urban coastline. Emphasis was given to the conservation of momentum during the simulation, as its distribution in space and time is the main factor of the wave's effects on the coastline. Due to this, a hybrid simulation method was adopted, based on the Smoothed Particle Hydrodynamics method, enriched with geometric constraints and rigid body interactions. The implementation is the result of cooperation between the Bullet physics engine and a custom SPH engine, which successively process the dynamic state of the fluid at every timestep of the simulation. Furthermore, in order to achieve better performance a custom data structure (LP grid) was developed for the optimization of locality in data storage and minimization of access time. Simulation data is exported to VTK files to allow interactive processing and visualization.

Keywords: Fluid simulation, tsunami, SPH, tsunami-coastline interaction, force visualization

1 Introduction

Simulations of natural phenomena are a precious tool for analysis and understanding of the processes behind them as well as the implications of those. Especially fluid dynamics is one of the fields most benefitted by the explosion of high performance parallel computing architectures of the last years. Tsunamis are one of the most devastating natural disasters, with much attention drawn to them lately, especially after the 2004 Indian Ocean tsunami and the 2011 Tōhoku earthquake and tsunami, two of the largest incidents of modern history. Multiscale modelling of tsunami generation, propagation and impact is a trending research area as respective simulations give valuable insights into the underlying mechanisms and relations between the various stages of an unfolding tsunami incident, while also facilitating the assessment of potential hazard it poses upon impact on a coastline.

A tsunami is a series of waves in a water body caused by an impulsive disturbance that vertically displaces a large volume of water. Tsunamis are generated by earthquakes, volcanic eruptions, landslides and other such events which have the potential to transmit a huge amount of mechanical energy to a water column. At large scales, tsunami propagation in the ocean is usually modelled through various versions of the Shallow Water Equations, derived from the Navier-Stokes equations in the case where the horizontal length scale is much greater than the vertical one. Conversely, simulations of tsunami impact is usually carried out using other methods, since complex dynamics must be taken into account. One of the most used methods for simulating complex flows with multiple boundary interactions is Smoothed Particle Hydrodynamics, initially proposed in the 1970s for the treatment of compressible flows in astrophysical problems. Since then, it has been applied to a wide variety of fields such as aerodynamics, geology, computer graphics and engineering with exceptional results. In our simulation, emphasis was given to the conservation of momentum and its distribution upon the coastline during the tsunami impact. Therefore, we adopted SPH as our method of choice due to the unparalleled advantages it offers, relating to its properties as lagrangian method.

2 Related Work

Computational fluid dynamics is a very active area of research, as it relates to a wide spectrum of applications in computer graphics, engineering and science. The SPH method was developed independently by Gingold and Monaghan [7] and Lucy [10] in 1977. Since then it has been employed in a wide variety of problems and applications, proving itself to be a flexible and attractive method for the simulation of complex, multicomponent/multiphase flows. Its flexibility is shown by the numerous adaptations and customizations it has undergone to suit many diverse problem domains.

Relating to the method itself, Desbrun and Gascuel [5] used the method to animate highly deformable bodies of various stiffness and viscosity, while proposing important extensions like the "spiky" pressure smoothing kernel and discussing implementation issues such as the surface reconstruction from density isosurfaces. Later, Müller et al. [12] used this work as a basis for fluid simulation in interactive applications. Becker and Teschner [2] developed Weakly Compressible SPH, where the ideal gas equation of state is replaced with the much more strict Tait equation to reduce compressibility to a user-defined upper bound, thus avoiding an inefficient explicit Poisson equation solver. In recent years, Solenthaler and Pajarola [13] improved WCSPH by proposing Predictive-Corrective Incompressible SPH, where a prediction-correction scheme is used to compute particle pressures through iterative density constraint satisfaction and propagation through the fluid, until the final tolerance conditions are met. Implicit Incompressible SPH was then proposed by Ihmsen et al. [8], in which the density is predicted using a discretized form of the pressure Poisson equation, as obtained from the combination of a direct discretization of the continuity equation and symmetric pressure forces.

Due to its adaptability and generality, SPH has been the method of choice for many applications and relative extensions. Macklin and Müller [11] enriched SPH with positional geometric constraints, thus enforcing incompressibility while maintaining stability and allowing for large timesteps. Rigid-fluid interaction is one of the strong aspects of the method, as is shown by Akinci et al. [1], where rigid surfaces are sampled by boundary particles, which adaptively contribute to fluid properties to address boundary region deficiencies and inhomogeneities, in order to incorporate rigid bodies to a unified hydrodynamic framework. Debroux et al. [4] used SPH for the simulation of tsunami impact on real coastline topography, where important features like the energy and speed of the wave were measured over the course of time. Finally, a thorough overview of various implementation algorithms and data structures together with their advantages and drawbacks is provided by Domínguez et al. [6].

3 Proposed framework

Our proposed simulation framework is based on SPH, a lagrangian fluid simulation method whose core notion is the discretization of the fluid into particles, which serve as interpolation points for the estimation of fluid properties in space. Advantages of this method include the exact treatment of advection, the natural way of dealing with special interface interactions, the inherent conservation of significant quantities (mass, momentum, energy) and the self-adaptivity of computational load to the fluid location and state in the flow domain. To efficiently ensure compressibility in degenerate cases and undersampled boundary regions while maintaining relatively large timesteps, SPH was enhanced with explicit solving of geometric constraints between particles. These constraints are solved by the Bullet physics engine, within which fluid particles are represented as rigid bodies, while also being subject to SPH forces as computed at each timestep of the simulation.

3.1 SPH method

Starting from the identity:

$$f(\boldsymbol{r}) = \int_V f(\boldsymbol{x})\delta(\boldsymbol{r}-\boldsymbol{x})d\boldsymbol{x},$$

where $\delta(\boldsymbol{r})$ the Dirac delta function and $\boldsymbol{x} \in V$, one can obtain a more general interpolation rule by substituting $\delta(\boldsymbol{r})$ with a smoothing kernel $W(\boldsymbol{r}, h)$:

$$f(\boldsymbol{r}) \approx \int_V f(\boldsymbol{x})W(\boldsymbol{r}-\boldsymbol{x}, h)d\boldsymbol{x}$$

whose limit when $h \to 0$ approaches the delta fucntion and is normalized to unity:

$$\lim_{h\to 0} W(\boldsymbol{r}, h) = \delta(\boldsymbol{r}) \quad \text{and} \quad \int_V W(\boldsymbol{r}, h)d\boldsymbol{x} = 1$$

The smoothing radius h serves as a cutoff radius in the smoothing process, as particles beyond that distance have no contribution to the sum, i.e. $W(r, h) = 0$ when $r > h$. For the discrete case, where f is discretized to particles with density

ρ and mass m, the weighting ratio m/ρ can be used to construct a weighted sum interpolant for any field A:

$$A(\boldsymbol{r}) = \sum_i \frac{m_i}{\rho_i} A(\boldsymbol{r}_i) W(\boldsymbol{r} - \boldsymbol{x}_i, h) \tag{1}$$

which lies at the heart of SPH formulation. According to this, the gradient can be computed by the following approximation:

$$\nabla A(\boldsymbol{r}) = \sum_i \frac{m_i}{\rho_i} A(\boldsymbol{r}_i) \nabla W(\boldsymbol{r} - \boldsymbol{x}_i, h) \tag{2}$$

The obvious advantage of this is the exclusive dependence on the smoothing kernel gradient, which can be precomputed for sensible kernel choices. However, this formula can lead to unsymmetric pair forces, compromising the conservation of linear and angular momentum of the system. To symmetrize these forces depending on gradients (like those originating from pressure differences), we can use the product rule:

$$\nabla \left(\frac{P}{\rho}\right) = \frac{\nabla P}{\rho} - \frac{P}{\rho^2}\nabla\rho \quad \Leftrightarrow \quad \nabla P = \rho \left[\frac{P}{\rho^2}\nabla\rho + \nabla\left(\frac{P}{\rho}\right)\right]$$

to obtain an alternative approximation of gradient

$$\begin{aligned} \nabla P &= \rho \left[\frac{P}{\rho^2} \sum_i \frac{m_i}{\rho_i} \rho \nabla W(\boldsymbol{r} - \boldsymbol{r}_i, h) + \sum_i \frac{m_i}{\rho_i} \frac{P_i}{\rho_i} \nabla W(\boldsymbol{r} - \boldsymbol{r}_i, h)\right] \\ &= \rho \sum_i m_i \left(\frac{P}{\rho^2} + \frac{P_i}{\rho_i}\right) \nabla W(\boldsymbol{r} - \boldsymbol{r}_i, h) \end{aligned} \tag{3}$$

which is antisymmetric for all interacting particle pairs. Viscosity forces on the other hand, are proportional to the laplacian of the velocity field:

$$\nabla^2 \boldsymbol{v} = \sum_i \frac{m_i}{\rho_i} (\boldsymbol{v}_i - \boldsymbol{v}) \nabla^2 W(\boldsymbol{r} - \boldsymbol{r}_i, h) \tag{4}$$

and are always antisymmetric, since they depend on velocity difference $\boldsymbol{v}_i - \boldsymbol{v}$ between particles. In each timestep of the simulation, the density of all particles is first computed according to equation 2, as it depends only on the relative position of those. The pressure at each particle location is then obtained from its respective density through an equation of state. Subsequently, the pressure and viscosity forces are computed from the particle data and integrated back into the position and velocity of the particles.

3.2 Implementation

Each simulation under our implementation consists of two elements, the coastline terrain (static) and the tsunami wave (dynamic). For the simulation setup, terrain is imported from a suitable 3D geometry definition file format, the initial conditions of the impacting wave (position and velocity) are configured, and the desired discretization resolution for the fluid is set. From these conditions, the terrain and fluid are initialized, and key parameters are computed as subsequently described. Terrain geometry is scaled by a user-supplied factor and docked to the origin of coordinates, while fluid particles are initially placed into an Hexagonal Close-Packed lattice, to achieve the densest possible packing and symmetry:

$$[x, y, z] = \left[2i + [(j+k) \bmod 2], \sqrt{3}[j + \frac{1}{3}(k \bmod 2)], \frac{2\sqrt{6}}{3}k \right] r \tag{5}$$

In this configuration, the smoothing radius h is computed such that each particle has approximately 50 neighbours (following the empirical rule established in the literature). The timestep is determined according to the Courant-Friedrichs-Lewy criterion:

$$\delta t_{\mathrm{CFL}} = C \frac{\delta x}{v_{\max}}, \tag{6}$$

for values of Courant number $C \approx 0.5$ with characteristic length δx equal to the effective particle radius and maximum velocity $v_{\max}$ determined by the maximum potential energy in the initial configuration. Following standard practice, we used three different smoothing kernels for density, pressure gradient and velocity laplacian computation:

$$W_{\mathrm{poly6}}(r, h) = \frac{315}{64\pi h^9} \begin{cases} (h^2 - r^2)^3 & 0 \leq r \leq h \\ 0 & \text{otherwise} \end{cases} \tag{7}$$

$$W_{\mathrm{spiky}}(r, h) = \frac{15}{\pi h^6} \begin{cases} (h - r)^3 & 0 \leq r \leq h \\ 0 & \text{otherwise} \end{cases} \tag{8}$$

$$\nabla W_{\mathrm{spiky}}(r, h) = \frac{-45}{\pi h^6}(h - r)^2$$

$$W_{\mathrm{viscosity}}(r, h) = \frac{15}{2\pi h^3} \begin{cases} -\frac{r^3}{2h^3} + \frac{r^2}{h^2} + \frac{h}{2r} - 1 & 0 \leq r \leq h \\ 0 & \text{otherwise,} \end{cases} \tag{9}$$

$$\nabla^2 W_{\mathrm{viscosity}}(r, h) = \frac{45}{\pi h^6}(h - r)$$

For the computation of the pressure from the estimated fluid density, the ideal gas equation of state is used:

$$P = k(\rho - \rho_0), \tag{10}$$

according to which the pressure is proportional to the difference of the current from the rest density. The major problem with this equation of state are the compressibility issues that have been shown to exist in simulations using it. A frequently proposed solution is to replace the above with the Tait equation of state:

$$P = B\left(\left(\frac{\rho}{\rho_0}\right)^{\gamma} - 1\right), \tag{11}$$

where usually $\gamma = 7$ and B a proportionality constant controlling the tolerance to density fluctuations. This equation is much more punishing on density fluctuations away from the rest density, therefore requiring significantly smaller timesteps to ensure stability. Here we follow a different approach, inspired by Position Based Dynamics, in which particles are represented by spherical rigid bodies. The most important advantage of this technique is the elegant handling of boundary, undersampled and degenerate fluid regions that tend to arise very frequently in simulations of free flows. The adoption of this approach allows to treat boundary collisions in a simple manner, while naturally enforcing incompressibility near boundaries and free surfaces. In these regions, estimators fail to describe the actual flow regime due to neighbour particle shortage. This undersampling creates the need for correction procedures, usually involving ghost/boundary particles, to avoid pressure instabilities, particle clustering and other artifacts. On the contrary, no such method is necessary under our representation, where degenerative cases are handled through geometric constraints thus selectively preventing unreliable estimations from affecting the flow.

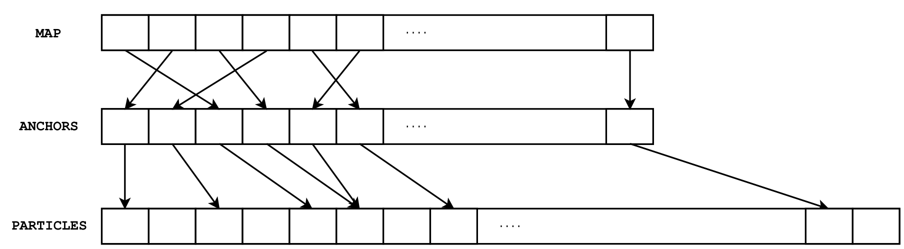

Fig. 1. Organization of the custom data structure designed for the efficient storing and interaction scanning between simulation particles. Top-down, the first vector implements the 3D to linear locality preserving mapping of cell anchors onto the second, which in turn points to each cell's particles on the third.

The Bullet physics engine is used to handle the rigid body dynamics. The simulation domain is divided by a regular grid of spacing equal to the smoothing radius into cells containing the fluid particles, which are generated as Bullet objects and stored in a custom cell list data structure consisting of three vectors. As shown in figure 1, particles are accessed by following pointers through those vectors in order, with the first encoding the 3D to linear locality preserving mapping of cells on the second, and the second pointing at first of the cell's particles which are continuously stored on the third, a dynamic sliding vector. This data structure allows for quick neighbour search, interaction scanning, exploitation of access patterns of the SPH algorithm and fast, in-place update. Simulation is following the Bullet framework, with the SPH code being embedded as an internal timestep tick callback function. We took advantage of the Bullet infrastructure to extract detailed information about the collisions between fluid and terrain regarding the resulting impulse, time, and location. Impulse and particle data are then written to multiple VTK files per frame. Samples of the smoothed color field (common name in the literature for the field having the value 1 at particle locations and 0 everywhere else) on the regular cell lattice are also exported, which are then used to reconstruct the fluid surface as an isosurface of that field. At the end of the simulation a cumulative impulse heatmap along with the scaled and docked terrain model are also provided.

4 Results

Multiple simulations were carried out using different models of urban coastline, in order to gain a significant and diverse dataset of impulses exerted over the duration of the impact. Tsunamis are vastly different from the usual wind-induced sea waves in that they have far longer wavelength and carry much greater total energy, appearing as a rapidly rising tide instead of a breaking waves. Accounting for these facts, we chose to represent the tsunami wave as a water volume invading the coastline with an initial velocity.

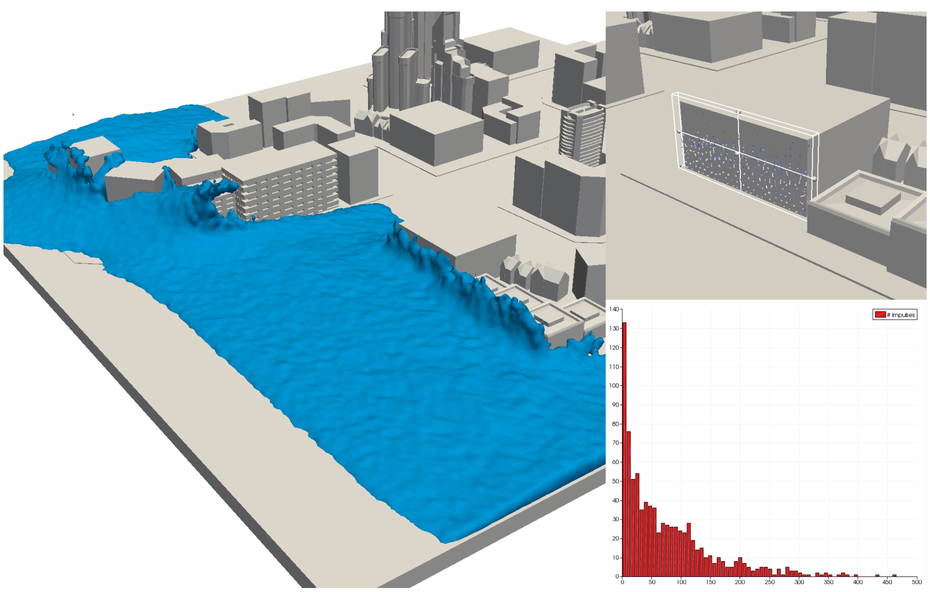

Fig. 2. Example visualization of impact data in Paraview$^{\mathrm{TM}}$. Fluid surface is reconstructed as isosurface of fluid density, while impulses on the selected region are visualized as points on the 3D terrain model and in a histogram grouped by their magnitude.

Figure 2 shows a typical simulation result with the aid of Paraview^{TM}, where the reconstructed wave surface and impulses exerted on a selected region are visualized along the 3D terrain model and plotted on a histogram. A comparison of the resulting impulse heatmap from the same tsunami impact upon an exposed model and one with a protective seawall is shown in figure 3. These heatmaps confirm a well-documented observation in the literature, i.e. that tsunami energy is absorbed mostly by the first obstacle in its way. This has been noted by Danielsen et al. [3] and Kathiresan and Narayanasamy [9], who both emphasized the protective role coastal vegetation (mangrove forests) played in mitigating the impact effects of the 2004 Indian Ocean tsunami. The same conclusion has been reached by Yanagisawa et al. [14] through theoretical approximation of the phenomenon backed by relevant field data and measurements. Seawalls have been constructed in high-risk regions as a common countermeasure against tsunami hazards. Although the waves may be so large as to overtop such barriers, these cases are somewhat rare, making seawalls an effective first line of defense.

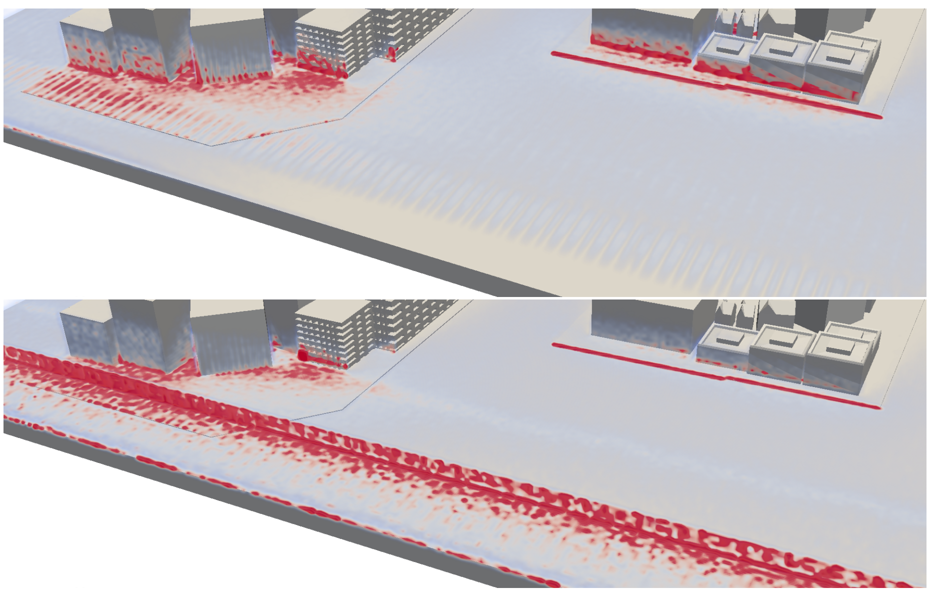

Fig. 3. Comparison between the impulse heatmap of a tsunami hit on the same urban coastline model, with (up) and without (down) the protection from a seawall. Seawalls are commonly found in high-risk areas, as they reduce impact effects significantly.

The performance of the simulation program was satisfactory, there is however a substantial margin for improvement. Figure 4 shows a plot of the mean computation time per output frame for variable fluid resolution. It is important to note that a higher number of simulation particles imposes a shorter internal timestep due to their smaller effective radius. These measurements are also representative of the worst-case scenario, as due to the initial fluid conditions the particles are closely packed in a single body of fluid, thus having maximum number of mutual interactions and reducing the performance gains from our spatial hashing data structure. About 75% of runtime is spent in single-threaded code consisting mostly of Bullet and I/O operations and while the rest in multi-threaded code of our SPH engine.

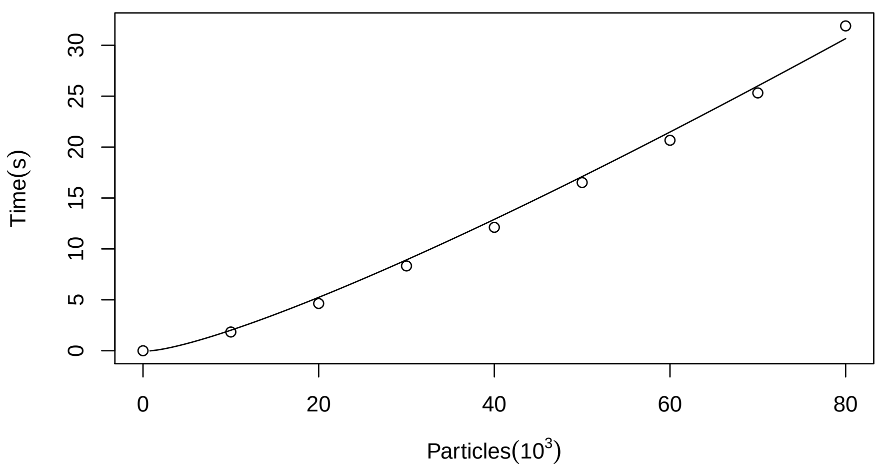

Fig. 4. Plot showing the mean simulation time required per output frame for the simulation of the first 10 frames, for 10k to 80k particles (continuous line represents $O(nlog_2n)$ growth).

5 Conclusions

References

1. Akinci, N., Ihmsen, M., Akinci, G., Solenthaler, B., Teschner, M.: Versatile rigid-fluid coupling for incompressible SPH. ACM Transactions on Graphics (TOG) 31(4), 62:1–62:8 (2012)
2. Becker, M., Teschner, M.: Weakly compressible SPH for free surface flows. In Proceedings of the 2007 ACM SIGGRAPH/Eurographics symposium on Computer animation, 209–217 (2007)
3. Danielsen, F., Sørensen, M. K., Olwig, M. F., Selvam, V., Parish, F., Burgess, N. D., Hiraishi, T., Karunagaran, V. M., Rasmussen, M. S., Hansen, L. B. and Quarto, A.: The Asian tsunami: a protective role for coastal vegetation. Science(Washington) 310(5748), 643 (2005)

4. Debroux, F., Prakash, M., Cleary, P.: Three-dimensional modelling of a tsunami interacting with real topographical coastline using Smoothed Particle Hydrodynamics. Proceedings of the 14th Australasian Fluid Mechanics Conference, Adelaide, Australia, 311–314 (2001)
5. Desbrun M., Cani, M. P.: Smoothed particles: A new paradigm for animating highly deformable bodies. In Computer Animation and Simulation 96 (Proceedings of EG Workshop on Animation and Simulation), 61–76 (1996)
6. Domínguez, J. M., Crespo, A. J., Gómez-Gesteira, M., Marongiu, J. C.: Neighbour lists in smoothed particle hydrodynamics. International Journal for Numerical Methods in Fluids 67(12), 2026–2042 (2011)
7. Gingold, R. A., Monaghan, J. J.: Smoothed particle hydrodynamics: theory and application to non-spherical stars. Monthly notices of the royal astronomical society 181(3), 375–389 (1977)
8. Ihmsen, M., Cornelis, J., Solenthaler, B., Horvath, C., Teschner, M.: Implicit incompressible SPH. Visualization and Computer Graphics, IEEE Transactions on 20(3), 426–435 (2014)
9. Kathiresan, K., Rajendran, N.: Coastal mangrove forests mitigated tsunami. Estuarine, Coastal and Shelf Science 65(3), 601–606 (2005)
10. Lucy, L. B.: A numerical approach to the testing of the fission hypothesis. The astronomical journal 82, 1013–1024 (1977)
11. Macklin, M., Müller, M.: Position Based Fluids. ACM Trans. Graph. 32(4), 104:1–104:12 (2013)
12. Müller, M., Charypar, D., Gross, M.: Particle-based fluid simulation for interactive applications. Proceedings of the 2003 ACM SIGGRAPH/Eurographics symposium on Computer animation, 154–159 (2003)
13. Solenthaler, B., Pajarola, R.: Predictive-corrective incompressible SPH. In ACM transactions on graphics (TOG) 28(3) 40:1–40:6 (2009)
14. Yanagisawa, H., Koshimura, S., Goto, K., Miyagi, T., Imamura, F., Ruangrassamee, A., Tanavud, C.: The reduction effects of mangrove forest on a tsunami based on field surveys at Pakarang Cape, Thailand and numerical analysis. Estuarine, Coastal and Shelf Science 81(1), 27–37 (2009)